Integrative paleophysiology of the metriorhynchoid Pelagosaurus typus (Pseudosuchia, Thalattosuchia)

Jorge Cubo, Mariana Sena, Romain Pellarin, Mathieu Faure-Brac, Paul Aubier, Cassandra Cheyron, Stéphane Jouve, Ronan Allain, Nour-Eddine Jalil

Received: 19 April 2024 | Revised: 10 July 2024 | Accepted: 12 July 2024

DOI: 10.1002/ar.25548

SPECIAL ISSUE ARTICLE

The Anatomical Record WILEY

Integrative paleophysiology of the metriorhynchoid *Pelagosaurus typus* (Pseudosuchia, Thalattosuchia)

Jorge Cubo[1] | **Mariana V. A. Sena**[1] | **Romain Pellarin**[1] | **Mathieu G. Faure-Brac**[2] | **Paul Aubier**[1] | **Cassandra Cheyron**[1] | **Stéphane Jouve**[1] | **Ronan Allain**[3] | **Nour-Eddine Jalil**[3]

[1]Sorbonne Université, Muséum National d'Histoire Naturelle, CNRS, Centre de Recherche en Paléontologie—Paris (CR2P, UMR 7207), Paris, France

[2]Naturhistorisk Museum, Universitetet i Oslo, Norsk Senter for Paleontologi, Oslo, Norway

[3]Muséum National d'Histoire Naturelle, Sorbonne Université, CNRS, Centre de Recherche en Paléontologie—Paris (CR2P, UMR 7207), Paris, France

Correspondence
Jorge Cubo, Sorbonne Université, Muséum National d'Histoire Naturelle, CNRS, Centre de Recherche en Paléontologie—Paris (CR2P, UMR 7207), Paris, France.
Email: jorge.cubo_garcia@sorbonne-universite.fr

Abstract

Paleophysiology is an emergent discipline. Organismic (integrative) approaches seem more appropriate than studies focusing on the variation of specific features because traits are tightly related in actual organisms. Here, we used such an organismic approach (including lifestyle, thermometabolism, and hunting behavior) to understand the paleobiology of the lower Jurassic (Toarcian) thalattosuchian metriorhynchoid *Pelagosaurus typus*. First, we show that the lifestyle (aquatic, amphibious, terrestrial) has an effect on the femoral compactness profiles in amniotes. The profile of *Pelagosaurus* indicates that it was amphibious, with a foraging activity in shallow marine environments (as suggested by the presence of salt glands) and thermoregulatory basking behavior in land (as suggested by the presence of osteoderms with highly developed ornamentation). As for the thermometabolism, we show that the mass-independent resting metabolic rate of *Pelagosaurus* is relatively high compared to the sample of extant ectothermic amniotes, but analysis of vascular canal diameter and inferences of red blood cell size refute the hypothesis suggesting incipient endothermy. Finally, the foraging behavior was inferred using two proxies. *Pelagosaurus* had a mass-independent maximum metabolic rate and an aerobic scope higher than those measured in the almost motionless *Iguana iguana*, similar to those measured in the sit-and-wait predator *Crocodylus porosus* but lower than those quantified in the active hunter *Varanus gouldii*. These results suggest that *Pelagosaurus* may have had a hunting behavior involving a slow sustained swimming or a patient waiting in shallow waters, and may have caught preys like gharials, using fast sideways sweeping motions of the head.

KEYWORDS

Crocodylomorpha, paleohistology, paleophysiology

1 | INTRODUCTION

Paleophysiological studies usually focus on specific features, namely the resting (e.g. Cubo et al., 2020; Faure-Brac & Cubo, 2020; Legendre et al., 2016) or the maximum (e.g., Knaus et al., 2021; Sena et al., 2023; Seymour et al., 2012) metabolic rates, blood flow index (Hu et al., 2023, 2024; Newham et al., 2020), genome size (Gardner et al., 2020; Organ et al., 2007; Organ & Shedlock, 2009), red blood cell size (Cubo et al., 2023; Faure-Brac et al., 2022, 2024; Huttenlocker & Farmer, 2017), body temperature (Bernard et al., 2010; Faure-Brac et al., 2022; Pochat-Cottilloux et al., 2023; Séon et al., 2020), blood pressure (Seymour, 2016; Seymour & Lillywhite, 2000), mineralized tissue homeostasis and acid–base regulation (Janis et al., 2020), levels of lipoxidation end-products (Wiemann et al., 2022), and the thermomotility index (Araújo et al., 2022). However, organismic (integrative) approaches seem more appropriate because all these features are tightly related in actual organisms. Here, we used the latter to understand three aspects of the paleobiology of the Lower Jurassic (Toarcian) thalattosuchian metriorhynchoid *Pelagosaurus typus*.

1. Lifestyle is a relevant paleobiological feature to be elucidated prior to performing any paleophysiological inference. Thalattosuchia is a taxa of mainly marine crocodyliforms formed by two clades: teleosauroids and metriorhynchoids. The presence of a hypocercal tail fin, pectoral and pelvic paddle-like limbs, enlarged preorbital salt glands, and osteoporotic-like bone tissues, and the absence of osteoderms, suggests that metriorhynchids had a pelagic, fully marine lifestyle (Fernandez & Gasparini, 2008; Hua & de Buffrénil, 1996; Ősi et al., 2018; Spindler et al., 2021; Young et al., 2010). In contrast, the presence of osteoderms with developed ornamentation and the absence of both a hypocercal tail fin and pectoral and pelvic paddle-like limbs (Ősi et al., 2018; Pierce & Benton, 2006) suggest that the non-metriorhynchid metriorhynchoid *Pelagosaurus typus* had a relatively semi-aquatic lifestyle similar to some teleosauroids (Johnson et al., 2020). Thus the question to be solved is: was *Pelagosaurus typus* a pelagic organism that used to go out of the water only for reproduction like marine turtles, or was it semiaquatic and used to spend time out of the water for thermoregulatory basking like extant crocodiles (Clarac & Quilhac, 2019; Johnson, 1974; Johnson et al., 1976, 1978)? We analyzed the bone compactness profiles in order to obtain a more precise picture of the lifestyle of this taxon.
2. Thermometabolism is a key physiological feature because it is linked to a wide range of biological features (e.g., growth rate, nutrient and oxygen intakes, etc.; Faure-Brac et al., 2024). In extant amniotes, two different thermometabolic regimes occur: endothermy, the capacity for an organism to produce its own heat through metabolic pathways that do not involve muscular contraction, and ectothermy, the absence of this capacity (Bal & Periasamy, 2020; Faure-Brac et al., 2024; Grigg et al., 2022; Rowland et al., 2015). It has been suggested that archosaurs were primitively endothermic (Seymour et al., 2004, based on the finding that a complete separation of the systemic and the pulmonary blood flows may be primitive for archosaurs; Legendre et al., 2016 and Cubo & Jalil, 2019 based on paleohistological data linked to bone growth rate), and Metasuchia (Notosuchia + Neosuchia) were secondarily ectotherms (Cubo et al., 2020, 2023 and Faure-Brac et al., 2022, based on paleohistological data linked to red blood cell size and to bone growth rate, and Faure-Brac et al., 2022 and Pochat-Cottilloux et al., 2023, based on isotopic data linked to body temperature). However, the phylogenetic frame of this reversion remains elusive, especially because the ancestral condition of Thalattosuchia is ambiguous (Faure-Brac et al., 2022). Hua and de Buffrénil (1996, p. 715) wrote "Histological observations suggest that the Thalattosuchia were ecto-poikilotherms" based on the finding of a zonal pattern containing highly vascularized zones formed at relatively high growth rates and avascular annuli formed at very low rates of growth. However, Séon et al. (2020, p. 6) found that: "Based on the available isotopic dataset, it seems likely that teleosaurids retained a typical ecto-poikilothermic thermophysiology in agreement with their morphology and ecology, whereas metriorhynchids may have been endothermic, being able to raise their body temperature above the ambient one, and close to that of other warm-blooded marine reptiles. However, metriorhynchids could not have achieved efficient thermoregulation, as suggested from their varying body temperature along with varying sea surface temperatures." If metriorhynchids acquired an "unachieved" or "incomplete" endothermy (Séon et al., 2020), then it would be interesting to infer what was the thermometabolic status of the non-metriorhynchid metriorhynchoid *Pelagosaurus* to elucidate the primitive condition in Thalattosuchia. For this, we carried out inferences of mass-independent resting metabolic rates (RMRs) and of red blood cell size of this taxon, both being tightly linked to the thermometabolic regime (Faure-Brac et al., 2024; Huttenlocker & Farmer, 2017; Montes et al., 2007; Soslau, 2020).
3. The relationship between the foraging behavior and the thermometabolism is more complex than it may seem at first sight. Extant endothermic amniots

(mammals and birds) tend to show higher resting (Montes et al., 2007) and maximum (Seymour et al., 2012) metabolic rates than their ectothermic counterparts (non-avian sauropsids). Among the latter, active hunters (e.g., varanid lizards) show higher maximum metabolic rates (MMRs) than sit-and-wait ambush predators (e.g., Crocodylia) (Sena et al., 2023). Was *Pelagosaurus typus* a sit-and-wait predator or an active hunter? We performed inferences of the mass-independent MMR and of the metabolic scope to shed light on this question.

To sum-up, our study is three-aimed to: (1) infer the lifestyle of *P. typus* through its bone compactness, (2) elucidate its probable thermometabolic regime estimating the RMR and red blood cell size, and (3) estimate its levels of activity and shed light into its hunting behavior by inferring the MMR and aerobic scope.

2 | MATERIALS AND METHODS

We performed a CT-scan of the left femur (bone length: 92.24 mm) of *Pelagosaurus typus* Bronn, 1841 MNHN.F. RJN470 (Figures 1 and 2a) to measure nutrient foramina size sensu Hu et al. (2020) and to analyze diaphyseal compactness profiles sensu Quémeneur et al. (2013). Diagnosis is reliable because the complete skeleton was available (although partly reconstructed). This specimen comes from the "Argiles à poissons" at Curcy-sur-Orne (Toarcian, France). Moreover, we made diaphyseal longitudinal and cross thin sections of *Pelagosaurus typus* right femur MNHN.F.RJN463 (Figure 2b) to quantify the relative primary osteon area (RPOA) sensu Fleischle et al. (2018), renamed by Faure-Brac and Cubo (2020), cellular density sensu Cubo et al. (2012) and vascular canal size sensu Huttenlocker and Farmer (2017), as well as to analyze the compactness profile sensu Quémeneur et al. (2013). Bone length could not be measured because the bone was incomplete. This specimen comes from La Caine (Toarcian, France). Diagnosis taken from the label at the MNHN collection. The thin sections (MNHN-F-Histos 3271 to 3276) were deposited at the hard tissue collection of the Muséum national d'Histoire naturelle (MNHN) of Paris and are available upon request to its curator. Histological observations were performed using a Nikon Eclipse E600 POL microscope under linearly and cross-polarized light.

FIGURE 1 Dorsal view of *Pelagosaurus typus* MNHN.F. RJN470 exposed at the Paleontology Gallery of the Muséum national d'Histoire naturelle (Paris). The two rows of dorsal osteorderms placed on the right and left sides of the specimen show extensive ornamentation. © Lilian Cazes, MNHN.

FIGURE 2 *Pelagosaurus typus* material analyzed in this study. (a) Left femur MNHN.F.RJN470 in dorsal, anterior, ventral and posterior views (from left to right) analyzed using CT-scan © Philippe Loubry, MNHN. (b) Proximal right femur MNHN.F. RJN463, associated to ribs and osteoderms, in dorsal view, analyzed using paleohistology. © Lilian Cazes, MNHN.

2.1 | Body mass and individual age

The body mass (BM, kg) of *Pelagosaurus typus* MNHN.F. RJN470 was inferred using femur volume (measured on the 3D object reconstructed from the CT-scan) and the equation published by Woodward et al. (2025):

$$\mathrm{BM} = \exp(1.00848 \times \ln(\text{femur volume}) - 7.13320) \quad (1)$$

The confidence interval was computed using the "*predict*" function with the argument "interval = 'prediction'" from the stats R package using R software (R Core Team, 2023).

The minimum individual age of *Pelagosaurus typus* MNHN.F.RJN463 was computed by counting the lines of arrested growth in the femoral cross section (de Buffrénil, Quilhac, & Castanet, 2021). The ontogenetic status was inferred from the observation of the outer layer of bone tissue: the presence of primary osteons in the process of formation may indicate active growth in progress, whereas absence of osteons and presence of a thick avascular layer of parallel fibered bone may suggest that growth is approaching the asymptote.

2.2 | Bone compactness

We quantified three parameters of the bone compactness profiles of *Pelagosaurus typus* MNHN.F. RJN470 left femur (using a CT-scan virtual cross section) and of *Pelagosaurus typus* MNHN.F.RJN463 right femur (using a cross thin section). These are, according to the definitions by Quémeneur et al. (2013): "S is the reciprocal of the slope at the curve inflection point; it is proportional to the relative width of the transition zone between the medulla and the cortical regions"; "P is the position of the curve inflection point on the x-axis; it materializes the position of the transition area between the medulla and the cortical regions" and "Compactness" is the parameter indicating the global compactness of the section. For this, first, we took pictures of the sections, and we assembled them in order to produce a full picture of each section. Second, these full pictures were binarized (using a threshold grayscale of 219) to produce a black and white duplicate, black corresponding to the bone matrix and white to the lumen let by the medullary and the vascular cavities. Finally, these binarized duplicates were processed by BoneProfileR web server v.2.4 build 766 (Girondot & Laurin, 2003). As one of our sections was incomplete (MNHN.F.RJN463 right femur), we followed the procedure described in Gônet et al. (2021) and removed a pie chart from the centroid.

Quémeneur et al. (2013) analyzed the bone compactness profiles of a sample of 155 species of extant amniotes of known lifestyle (aquatic, amphibious, terrestrial) and constructed an inference model using a discriminant analysis. Please note that these authors based their analyses only on adult specimens (see the Caveats section for the implications on our study). Fabbri et al. (2022) used phylogenetically flexible discriminant analyses to infer lifestyle in carnivorous dinosaurs. As the discriminant analysis approach has been criticized (Myhrvold et al., 2024), we used *t* tests to infer the lifestyle of *Pelagosaurus typus* by checking whether the femoral compactness parameters of MNHN.F.RJN470 left femur and of MNHN.F.RJN463 right femur are significantly different from the means of extant aquatic and amphibious groups. We checked previously whether the lifestyle is a factor explaining the variation of parameters of the femoral compactness profiles in amniotes

using a phylogenetic ANOVA and the dataset published by Quémeneur et al. (2013) to which we added three species of Crocodylia (*Alligator mississippiensis* MNHN-F-Histos 2953; *Crocodylus niloticus* MNHN-F-Histos 2967 et 2968; et *Gavialis gangeticus* MNHN-F-Histos 3201; thin sections are available at the hard tissue collection of the Paris MNHN).

2.3 | Resting metabolic rate

We constructed an inference model using a sample of extant species for which both (i) the proxies (the osteocyte density and RPOA), and (ii) the RMRs were available. We compiled a dataset of extant young amniotes using published datasets (Table 1), to which we added *Alligator mississippiensis* MNHN-F-Histos 2953.

The final sample is composed of 18 species (Table 1). Osteohistological measurements were performed in femora exclusively to carry out analyses in a strict frame of homology. Table 1 contains raw RMR values (mL O_2 h^{-1}). Readers can compute the mass-independent MMR values (mL O_2 h^{-1} g^{-b}) using their preferred b value (the exponent in the preceding expression) and the associated BM. Our analyses were performed using mass-independent RMRs computed using values of mL O_2 h^{-1} $g^{-0.67}$ to correct for the effect of increasing surface/volume ratio when decreasing BM, as suggested by Montes et al. (2007).

2.4 | Probability of endothermy

Huttenlocker and Farmer (2017) and Cubo et al. (2023) tested the relationship between red blood cell size and bone vascular canal diameter using a sample of, respectively, 14 and 30 species of extant tetrapods. Thus, bone vascular canal diameter can be used as a proxy of red blood cell size (linked to endothermy; Soslau, 2020) in amniotes. Consistently, Cubo et al. (2023) constructed a model using a sample of 46 species of extant tetrapods

TABLE 1 Dataset used to infer mass-independent resting metabolic rate.

Species	Body mass (g)	RMR (mL O_2 h^{-1})	RMR (mL O_2 h^{-1} $g^{-0.67}$)	Osteocyte density (osteocyte lacunae/µm²)	RPOA
Alligator mississippiensis	750.00 (1)	12.525 (1)	0.148 (1)	0.0008 (2) (11)	0.164 (2)
Anas platyrhynchos	109.75 (3)	258.120 (3)	11.085 (3)	0.0026 (4)	0.583 (5)
Caiman crocodilus	749.00 (1)	10.118 (1)	0.120 (1)	0.0010 (6)	0.137 (6)
Capreolus capreolus	7000.00 (7)	3972.870 (7)	10.541 (7)	0.0050 (8) (11)	0.735 (5)
Cavia porcellus	100.00 (3)	76.100 (3)	3.478 (3)	0.0019 (4)	0.336 (5)
Chelodina oblonga	23.85 (3)	0.730 (3)	0.087 (3)	0.0010 (4)	0.000 (5)
Crocodylus niloticus	215.33 (3)	11.500 (3)	0.314 (3)	0.0007 (4)	0.052 (5)
Gallus gallus	90.00 (3)	177.480 (3)	8.706 (3)	0.0025 (8)	0.682 (5)
Lepus europaeus	1031.00 (9)	1017.970 (9)	9.747 (9)	0.0049 (8) (11)	0.809 (5)
Microcebus murinus	14.60 (3)	9.200 (3)	1.526 (3)	0.0039 (4)	0.241 (5)
Mus musculus	5.08 (3)	5.070 (3)	1.706 (3)	0.0012 (4)	0.076 (5)
Oryctolagus cuniculus	450.00 (10)	607.500 (10)	10.137 (10)	0.0040 (8) (11)	0.422 (5)
Pelodiscus sinensis	5.77 (3)	0.270 (3)	0.083 (3)	0.0009 (4)	0.000 (5)
Podarcis muralis	1.08 (3)	0.080 (3)	0.076 (3)	0.0011 (4)	0.000 (5)
Trachemys scripta	16.13 (3)	0.700 (3)	0.109 (3)	0.0014 (4)	0.000 (5)
Varanus exanthematicus	46.00 (3)	2.030 (3)	0.156 (3)	0.0012 (4)	0.005 (5)
Varanus niloticus	32.50 (3)	3.110 (3)	0.302 (3)	0.0010 (4)	0.018 (5)
Zootoca vivipara	0.50 (3)	0.070 (3)	0.111 (3)	0.0024 (4)	0.000 (5)

Note: (1) Bennett and Dawson (1976); (2) this study, thin section femur MNHN-Histos 2953; (3) Montes et al. (2007); (4) Cubo et al. (2012); (5) Faure-Brac & Cubo (2020); (6) Cubo et al. (2020); (7) computed using data taken from Mauget et al. (1999): at the age of 6 weeks, the body mass is 7000 g and the RMR 2050 kJ/day; assuming that 1000 mL O_2 = 21.1 kJ; (8) Olivier et al. (2017); (9) computed using data taken from Hackländer et al. (2002): at weaning the body mass is 1031 g and the RMR 500 kJ/day kg; assuming that 1000 mL O_2 = 21.1 kJ; (10) computed using data taken from Seltmann et al. (2009): dry juvenile rabbits at 23°C with a mean body mass of 450 g had an RMR = 1.35 mL O_2/g h; (11) the RMRs were measured in youngs of a few weeks and the osteohistological data in adults. Thus, in the later, histological measurements were performed in the deep cortex formed when they were young (see "Caveats" section).

and phylogenetic logistic regressions (PLRs; Ives & Garland, 2010), to infer the probability of endothermy from bone vascular canal diameter. Both datasets are available in Dryad at Cubo et al. (2022). Here, we quantified the harmonic mean of vascular canal diameter of *Pelagosaurus typus* according to the protocol described in Huttenlocker and Farmer (2017), and used it to infer its probability of endothermy using the model published by Cubo et al.'s (2023):

$$\mathrm{p(endoth)} = \frac{\exp(-0.45 \times \mathrm{Canal\ size(\mu m)} + 6.04)}{1 + \exp(-0.45 \times \mathrm{Canal\ size(\mu m)} + 6.04)} \quad (2)$$

where p(endoth) is the probability of endothermy for an extinct organism given its harmonic mean vascular canal size (μm).

2.5 | Red blood cell size

To further investigate *Pelagosaurus* thermometabolism, we inferred red blood cell width using the dataset containing this variable plus bone vascular canal diameter published by Cubo et al. (2023) available in Dryad at Cubo et al. (2022).

2.6 | Maximum metabolic rate

An inference model was constructed using a sample of extant species for which both (i) the proxies (an index of blood flow, Q_i, cm^3; Seymour et al., 2012, and blood flow rate, $\dot{Q}$, $cm^3 s^{-1}$; Seymour et al., 2019), and (ii) the MMRs were available. For this, we expanded the dataset on MMR measurements and nutrient foramina size published by Seymour et al. (2012, $n = 19$ taxa) by adding data for 10 new species. For eight of them nutrient foramina were measured in specimens hosted at the Paris MNHN, and the corresponding MMRs and BMs were taken from the literature; Table 2). The remaining two additional species are: (i) *Crocodylus porosus* for which Seymour et al. (2012) provided the nutrient foramen size of a 470 kg BM specimen, and we estimated the corresponding MMR using the equation ($MMR = 6.56BM^{0.829}$) published by Seymour (2013); and (ii) *Crocodylus niloticus* MNHN-ZA-AC-2015-25 for which we measured the nutrient foramina, inferred the BM using femur length and the equation published by Woodward et al. (2025):

$$\mathrm{BM} = \exp(3.6427^{*}\ln(\mathrm{femur\ length}) - 14.66296) \quad (3)$$

TABLE 2 Dataset used to infer mass-independent maximum metabolic rate.

Species	MMR ($mL\ O_2\ h^{-1}$)	Mass (g)	Foramen radius (mm)	Femur length (mm)	Qi (mm^3) (1)	$\dot{Q}$ ($cm^3\ s^{-1}$) (2)
Acinonyx jubatus	64,908.00 (3)	28,100 (3)	0.513 (4)	250.83 (4)	0.0002762654667	0.1056115414
Alligator mississippiensis	10,512.00 (3)	53,000 (3)	0.312 (5)	175.15 (5)	0.0000541001	0.0309258
Amphibolurus barbatus	132.17 (6)	239 (6)	0.076 (7)	40.01 (7)	0.0000008339	0.0007485
Bettongia penicillata	11,682.00 (1)	1,018 (1)	0.194 (1)	79.61 (1)	0.0000173264000	0.0091548014
Bos taurus	1,453,500.00 (1)	225,000 (1)	0.777 (1)	390.00 (1)	0.0009349570000	0.2846363057
Capra hircus	806,820.00 (1)	45,000 (1)	0.480 (1)	196.00 (1)	0.0002702270000	0.0896899314
Chelonia mydas	70,963.20 (1)	115,000 (1)	0.242 (1)	47.63 (1)	0.0000745230000	0.0161887658
Crocodylus niloticus	14,810.91 (8)	79,527 (8)	0.151 (9)	185.33 (9)	0.0000027682	0.0047296
Crocodylus porosus	64,598.76 (8)	470,000 (1)	0.540 (1)	249.00 (1)	0.0003554420000	0.1197411846
Dasyuroides byrnei	1435.20 (1)	92 (1)	0.086 (1)	33.69 (1)	0.0000017554700	0.0010674906
Equus caballus	3,360,300.00 (1)	675,000 (1)	1.799 (1)	463.75 (1)	0.0244652890000	1.931572127
Helogale parvula	4,032.00 (3)	580 (3)	0.125 (10)	41.68 (10)	0.0000058361041	0.0028821347
Iguana iguana	318.00 (6)	795 (6)	0.12 (11)	83.30 (11)	0.0000024894	0.0025902
Isoodon obesulus	5,731.80 (1)	717 (1)	0.193 (1)	62.03 (1)	0.0000291277000	0.0091296143
Oryctolagus cuniculus	6,750.00 (1)	1,590 (1)	0.174 (1)	84.29 (1)	0.0000120300000	0.0069124158
Ovis aries	60,822.00 (1)	21,150 (1)	0.507 (1)	196.50 (1)	0.0003366720000	0.1025202182
Papio hamadryas	44,352.00 (3)	8,500 (3)	0.303 (12)	228.35 (12)	0.0000368027618	0.0286776263
Potorous tridactylus	7,344.00 (1)	976 (1)	0.122 (1)	79.03 (1)	0.0000028227000	0.0027066115
Sus scrofa	103,896.00 (1)	55,300 (1)	0.463 (1)	225.50 (1)	0.0002045200000	0.0821046620
Tachyglossus aculeatus	3,955.80 (1)	2,725 (1)	0.144 (1)	59.29 (1)	0.0000108138000	0.0041963740

(Continues)

TABLE 2 (Continued)

Species	MMR (mL O_2 h^{-1})	Mass (g)	Foramen radius (mm)	Femur length (mm)	Qi (mm^3) (1)	$\dot{Q}$ (cm^3 s^{-1}) (2)
Tiliqua rugosa	421.32 (1)	609 (1)	0.040 (1)	28.84 (1)	0.0000000959587	0.0001220708
Tiliqua scincoides	250.27 (1)	493 (1)	0.062 (1)	21.19 (1)	0.0000007176460	0.0004216165
Tupinambis teguixin	674.70 (13)	865 (13)	0.128 (14)	48.52 (14)	0.0000054465	0.0030458
Varanus gouldii	1,254.19 (1)	443 (1)	0.240 (1)	64.21 (1)	0.0000399368000	0.0159635094
Varanus mertensi	1,068.89 (1)	1,121 (1)	0.244 (1)	61.57 (1)	0.0000547876000	0.0166410749
Varanus panoptes	3,159.87 (1)	2,317 (1)	0.215 (1)	81.50 (1)	0.0000252219000	0.0119839621
Varanus salvator	8,352.00 (3)	7,700 (3)	0.683 (15)	106.71 (15)	0.002039322142	0.2099077748
Varanus varius	5,702.01 (1)	6,343 (1)	0.180 (1)	78.56 (1)	0.0000076862900	0.0075483198
Vulpes vulpes	50,364.00 (1)	4,440 (1)	0.303 (1)	127.77 (1)	0.0000687675000	0.02882140643

Note: Foramen radius was computed from area, assuming circularity, in data taken from Seymour et al. (2012) and in data produced in this study. When several nutrient foramina were present in a given bone we added the corresponding areas and computed the radius of the resulting value assuming circularity. (1) Seymour et al. (2012); (2) Seymour et al. (2019); (3) Pontzer et al. (2009); (4) this study, MNHN-JAC-1901-541; (5) this study, MNHN-ZA-AC-1919-113; (6) Bennett and Dawson (1976); (7) this study, MNHN-ZA-AC-1967-119; (8) this study, see methods; (9) this study, MNHN-ZA-AC-2015-25; (10) this study, MNHN-1987-176; (11) this study, MNHN-ZA-AC-1974-129; (12) this study, MNHN-1880-1163; (13) Crispin (2014); (14) this study, MNHN-ZA-AC-1967-96; (15) this study, MNHN-ZA-AC-1884-284. The Qdot values of the species of the sample are comparable among them (as they are all computed in the same way, assuming that artery lumen area equals nutrient foramen area) but these values are overestimations because in living animals artery lumen area is roughly 20% of the nutrient foramen area (Hu et al. 2021)

and estimated the corresponding MMR using the equation published by Seymour (2013).

The final sample is composed of 29 species (Table 2). Table 2 contains raw MMR values (mL O_2 h^{-1}) and BM. No consensus exists about the value of the exponent b of mass-independent MMR values (mL O_2 h^{-1} g^{-b}) to be used in comparative analyses. According to Seymour (2013), $b = 0.872$ in placental mammals and $b = 0.829$ in crocodiles. We decided to use the universal exponent $b = 0.67$ for three important reasons. First, we cannot mix different units (exponents) in the same analysis. Thus, it would be flawed to use in our predictive model the exponents $b = 0.872$ for placental mammals, $b = 0.829$ for crocodiles and a different exponent b for the other sauropsids of the sample. Second, to be able to compare the MMR and the RMR inferred for *Pelagosaurus*, and to compute its aerobic scope, both metabolic rates must be inferred in the same units. And third, Knaus et al. (2021) used it in a comparative study of MMR because "many metabolic processes in animals are dependent on surface area of body membranes, which correlate with BM to the power of 0.67." Thus, we used an exponent $b = 0.67$ but provided readers with raw MMR (mL O_2 h^{-1}) and BM (g) values (Table 2) so that, if necessary, they can compute the mass-independent MMR values (mL O_2 h^{-1} g^{-b}) using their preferred b exponent.

Nutrient foramina measurements were performed in a single skeletal element (femur) to carry out analyses in a strict frame of homology. We obtained a CT-scan of *Pelagosaurus typus* MNHN.F.RJN470 using the platform AST-RX of the Muséum national d'Histoire naturelle (Paris). The parameters were: voltage: 110 kV; current: 320 μA; exposition time: 333 ms; filter: 0.3—Cu mm; image pixel size: 142 μm; number of projections: 720. The segmentation and measurements of nutrient foramina were made in Mimics® Innovation Suite v.24 (Materialize). The foramina were drawn manually in sagittal, coronal and axial CT-scan slice views, and then imaged in 3D using the "Multiple slice edit" tool. Cross-sectional area of each foramen at the periosteal opening was measured using the "Area" tool. Finally, we computed the radius of the foramen applying the circle area equation. The bone length was measured using the "Distance" tool from the distal to the proximal extremities of the 3D object. These values were used to compute our two proxies to infer MMRs: (i) an index of blood flow (Q_i, cm^3) from foramen radius (r_i) and bone length (L) (Seymour et al., 2012):

$$Q_i = r_i^4 / L \quad (4)$$

and (ii) blood flow rate ($\dot{Q}$, cm^3 s^{-1}) from arterial lumen radius (r_i) (Seymour et al., 2019):

$$\log \dot{Q} = -0.20 \log r_i^2 + 1.91 \log r_i + 1.82 \quad (5)$$

2.7 | Phylogenies

We used the phylogenies compiled by Quémeneur et al. (2013), Legendre et al. (2016), Cubo et al. (2023) and Sena et al. (2023) as reference topologies for the compactness, the RMR, the red blood cell size and the MMR analyses

respectively, using phylogenetic comparative methods. As the samples have been expanded in this study, we produced supertrees manually by adding the new species to these phylogenies using the topologies by Pyron et al. (2013) for Squamata, Villa et al. (2018) for *Varanus*, Upham et al. (2019) for Mammalia, and Zurano et al. (2019) for Cetartiodactyla. These phylogenies were dated using TimeTree (Kumar et al., 2022; last access on January 31, 2024) for extant taxa, the Paleobiology Database for *Pelagosaurus typus* last appearance datum (last access on January 31, 2024) and de Buffrénil, Laurin, and Jouve (2021) to date the node Thalattosuchia—Neosuchia.

2.8 | Phylogenetic comparative methods

Paleobiological inference models of RMR, red blood cell size and MMR were constructed using phylogenetic eigenvector maps (PEMs; see Guénard et al., 2013, for a theoretical description and Legendre et al., 2016, for an empirical application) using the package "MPSEM" (Guénard et al., 2013) for R (R Core Team, 2023). These models allowed us to infer *Pelagosaurus* RMR, red blood cell size and MMR, and the corresponding 95% confidence intervals. The latter were useful to compare the inferred values to those measured in related extant species. The model to compute the probability of endothermy was constructed using PLRs (see Ives & Garland, 2010, for a theoretical description and Cubo et al., 2023, for an empirical application), using the package "phylolm" (Tung Ho & Ané, 2014) for R (R Core Team, 2023). Finally, the hypothesis of a link between the lifestyle (aquatic, amphibious or terrestrial) and the parameters of the bone compactness profiles was tested using phylogenetic ANOVA (see Garland et al., 1993, for a theoretical description and Mitchell et al., 2017 for an empirical study) using the package "phytools 2.0" (Revell, 2024) for R (R Core Team, 2023). Normality was tested for each variable and each group (aquatic, amphibious, terrestrial) using Shapiro Wilk tests. Homogeneity of variances (homoscedasticity) among these three groups was tested for each variable using Bartlett tests.

3 | RESULTS

3.1 | Individual age and BM

We inferred the BM of *Pelagosaurus typus* MNHN.F.RJN470 and the corresponding 95% confidence interval, using left femur volume (7474.95 mm^3) computed from the CT-scan, and the equation published by Woodward et al. (2025, see above). The value inferred is 6.435 kg (5.112–8.137 kg).

The BM of *Pelagosaurus typus* MNHN.F.RJN463 was slightly smaller as suggested by the comparison of femoral diaphyseal maximal diameters (11.49 vs. 10.01 mm). We inferred an individual age of at least 5 years for the latter specimen by counting the lines of arrested growth of the thin section (Figure 3a). Moreover, we know that this specimen was still growing, as suggested by the fact that the process of formation of primary osteons is still in action on bone periphery (Figure 3b).

3.2 | Bone compactness

The analysis of the compactness profile of *Pelagosaurus typus* MNHN.F.RJN470 left femur (CT-scan virtual cross-section) outputs the following values: S parameter = 0.057; P parameter = 0.566, and compactness = 0.647 (Figure 4a). The corresponding analysis for *Pelagosaurus typus* MNHN.F.RJN463 right femur (cross thin-section) outputs: S parameter = 0.061; P parameter = 0.566, and compactness = 0.690 (Figure 4b).

We tested whether the lifestyle (aquatic, amphibious, or terrestrial) is a factor explaining the parameters of the bone compactness profiles using the angular values of the dataset published by Quémeneur et al. (2013) (to which we added three Crocodylia), and phylogenetic ANOVA. For the S parameter of the compactness profile, neither normality (aquatic: $p = 0.00019$; amphibious: $p = 2.759e\text{-}05$; terrestrial: $p < 2.2e\text{-}16$) nor homoscedasticity ($p = 0.0003049$) were verified, so the phylogenetic ANOVA analysis could not be carried out. For the compactness, the group of aquatic species had a normal distribution ($p = 0.1867$) but normality was not verified in the amphibious ($p = 0.0001854$) nor in the terrestrial ($p = 0.0043$) groups. Homoscedasticity was not verified either for the compactness (0.03438). Therefore, phylogenetic ANOVA analysis could not be performed for this parameter either. In contrast, both normality (aquatic: $p = 0.5779$; amphibious: $p = 0.3796$; terrestrial: $p = 0.1363$) and homoscedasticity ($p = 0.6896$) were verified for the P parameter of the compactness profile. The phylogenetic ANOVA shows that lifestyle is a factor significantly explaining the variation of the P parameter ($p = 0.004$). The aquatic group had a mean P parameter of 0.394 and a 95% confidence interval of 0.316–0.471. The value measured in *Pelagosaurus typus* MNHN.F.RJN470 left femur and MNHN.F.RJN463 right femur (P parameter = 0.566 in both cases) is significantly higher than the mean value of the aquatic group ($p = 0.0003$). The amphibious group had a mean P parameter of 0.526 and a 95% confidence interval of 0.478–0.573. The value measured in *Pelagosaurus typus* is not significantly different from the mean value of the amphibious group ($p = 0.093$). Finally, the terrestrial group had a mean P parameter of 0.636 and a 95% confidence interval of 0.612–0.658. The value measured in *Pelagosaurus typus* is significantly lower than the mean value of the terrestrial group ($p = 1.536e\text{-}08$).

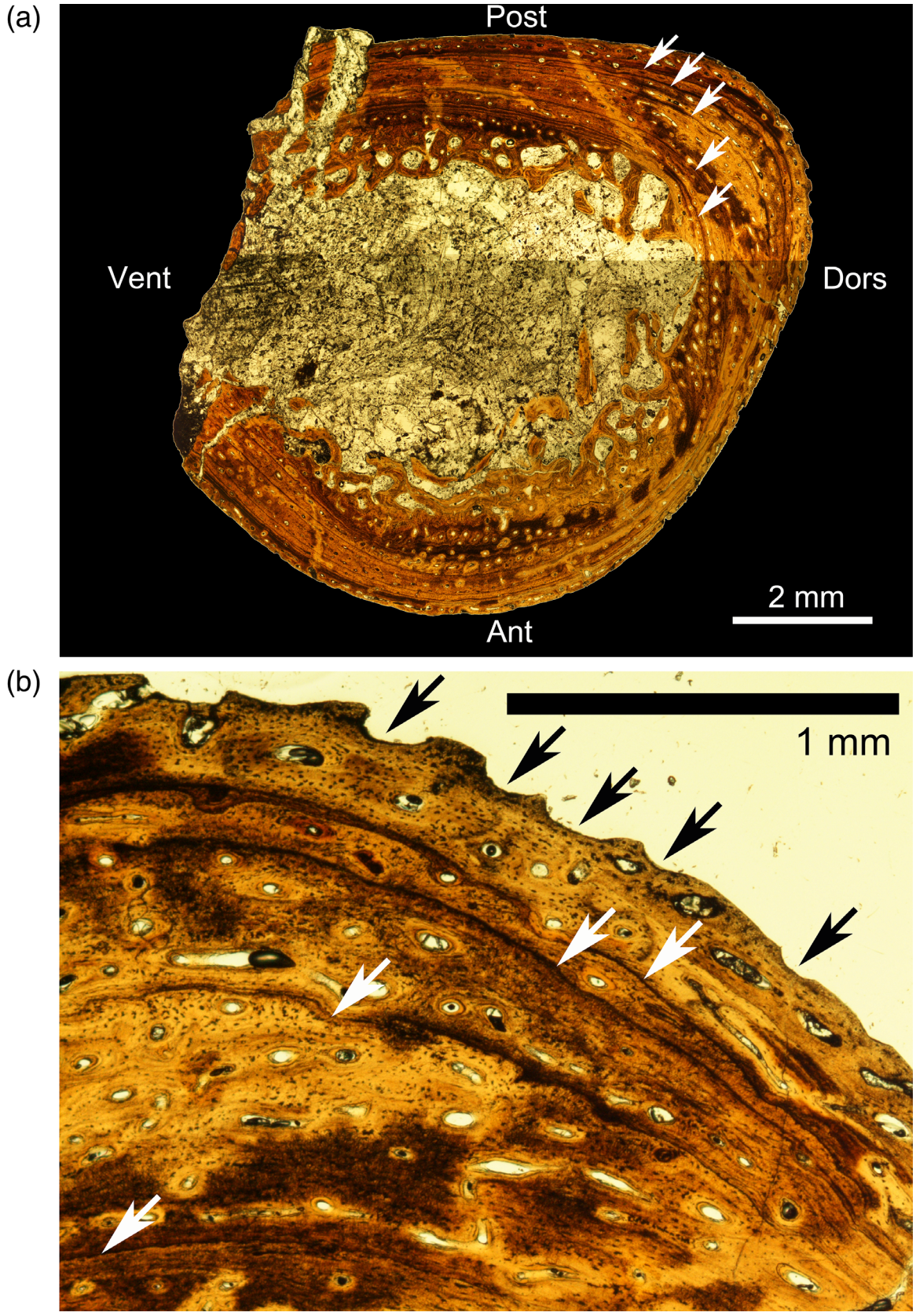

FIGURE 3 Diaphyseal cross section of the right femur of *Pelagosaurus typus* MNHN.F.RJN463. (a) Complete cross section showing at least five lines of arrested growth (white arrows). (b) Outer layer at the dorsal side showing the process of formation of primary osteons (black arrows).

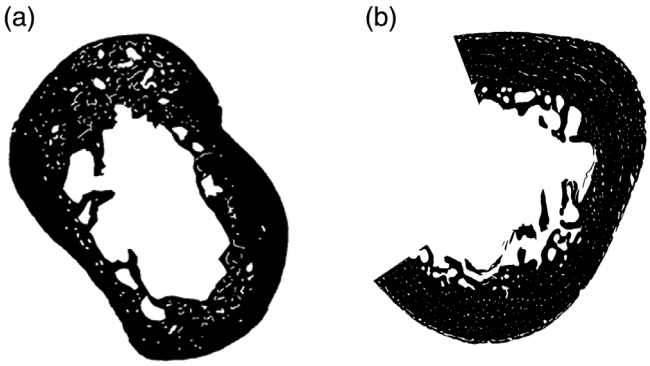

FIGURE 4 Drawings showing the bone tissue distribution on diaphyseal cross sections of (a) left femur MNHN.F.RJN470 and (b) right femur MNHN.F.RJN463 (this section is incomplete because the bone was broken at the diaphysis). Drawings are not to scale.

3.3 | Resting metabolic rate

We constructed a model to infer the RMR using PEM and two osteohistological explanatory variables: osteocyte density and RPOA (Table 1). The PEM method selects a subset of phylogenetic eigenvectors plus a single explanatory variable to avoid model overfitting. The model including osteocyte density had an AICc value of 2.830, and the model including RPOA an AICc value of −7.908. We chose the one with the lowest AICc value. The selected model included RPOA and the phylogenetic eigenvectors 1, 4, 10, 11, and 16 (p-value = $1.035e^{-10}$; adjusted $R^2 = 0.986$). Using this model, we inferred an RMR of 1.513 mL O_2 h^{-1} $g^{-0.67}$ (1.307–1.751 mL O_2 h^{-1} $g^{-0.67}$) for *Pelagosaurus typus* MNHN.F.RJN463 (Figure 5). A leave-one-out cross-validation test showed that, for extant species, predicted values are not significantly different from observed values ($p = 0.966$).

3.4 | Probability of ectothermy

We measured the vascular canal size sensu Huttenlocker and Farmer (2017), related to red blood cell size (Huttenlocker & Farmer, 2017, $n = 14$; Cubo et al., 2023,

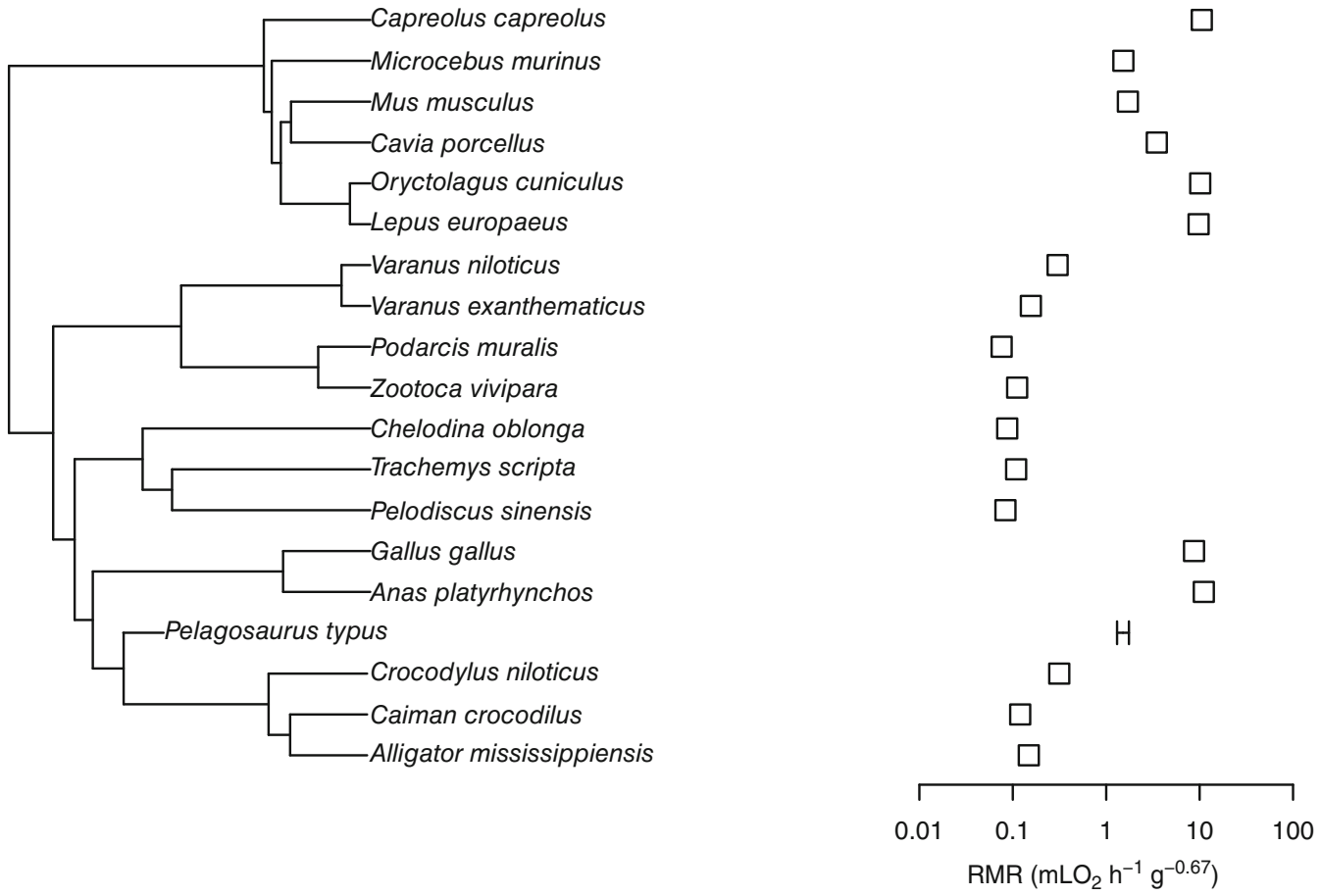

FIGURE 5 Mass-independent resting metabolic rates quantified in a sample of extant amniotes and inferred in *Pelagosaurus typus* using a set of phylogenetic eigenvectors and the relative area of primary osteons. Dataset available in Table 1.

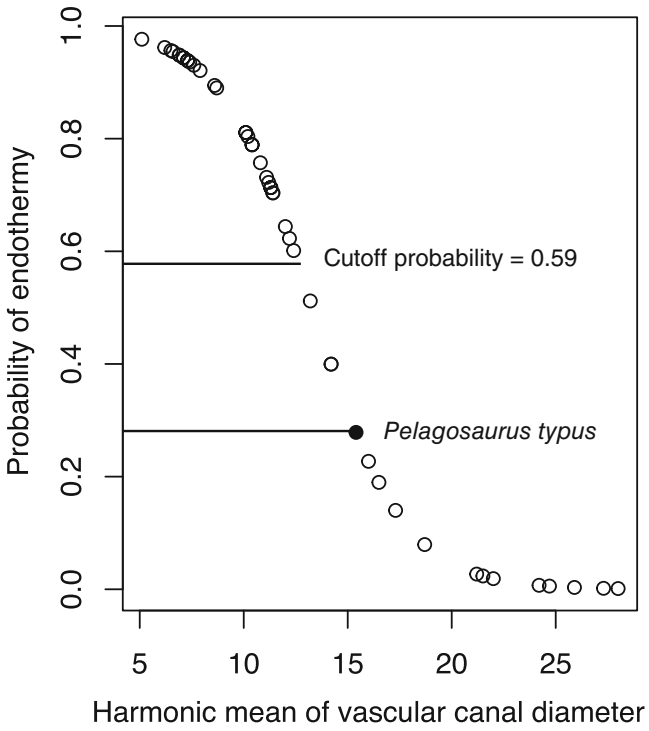

FIGURE 6 Phylogenetic logistic regression modeling the distribution of probabilities of being endothermic inferred for our sample of extant tetrapods using the harmonic mean of femoral vascular canal diameter as the explanatory variable (modified from figure 3 in Cubo et al., 2023).

$n = 31$), and obtained a harmonic mean of vascular canal diameter of 15.7 μm (SD = 0.51). We used this value to infer the probability of endothermy of *Pelagosaurus typus* with Equation 2 (this article) obtained by Cubo et al. (2023; n = 46) through PLR (Figure 6). We obtained a probability of endothermy of 0.27 (Figure 6). This value is lower than the cutoff probability of 0.59 separating endotherms from ectotherms (Cubo et al., 2023), so we conclude that *Pelagosaurus typus* MNHN.F.RJN463 had an ectothermic thermometabolism.

3.5 | Red blood cell size

We constructed a model including red blood cell sizes quantified in a sample of extant amniotes and inferred in *Pelagosaurus typus*, as well as a set of phylogenetic eigenvectors (1, 2, 6, 12, 13, 14, 19, and 25) and the harmonic mean of bone vascular canal diameter (sensu Huttenlocker & Farmer, 2017). Dataset analyzed by Cubo et al. (2023) available in Dryad at Cubo et al. (2022). The model was highly significant (p-value = $3.952e^{-11}$; adjusted $R^2 = 0.929$). Using this model, we inferred a red blood cell width of 8.76 μm (8.08–9.49 μm) for *Pelagosaurus typus* MNHN.F.RJN463 (Figure 7). This confidence interval excludes the value separating endotherms with small red blood cells from ectotherms with large ones (Figure 7).

3.6 | Maximum metabolic rate

We constructed a model to infer the MMR using PEM and two osteological explanatory variables: an index of blood flow (Q_i, cm^3) and blood flow rate ($\dot{Q}$, $cm^3\ s^{-1}$). *Pelagosaurus typus* MNHN.F.RJN470 had two nutrient foramina (Figure 8). We followed the path of both foramina from the periosteum to the endosteum and we confirm that, although they are metaphyseal, they are nutrient foramina. We performed segmentation of them using the CT-scan (Figure 8) and measured their cross-sectional areas and the corresponding radii (0.08 mm and 0.115 mm) at their periosteal openings as well as the femur length (92.24 mm). We added the two areas and computed the radius of the resulting value assuming circularity. The PEM model including Q_i had an AICc value of 35.859, and the model including $\dot{Q}$ an AICc value of 34.616. We chose the one with the slightly lower AICc value. This model included $\dot{Q}$ and the phylogenetic eigenvectors 1, 2, 3, 4, 5, 9, 10, 12, 15, 16, 21, and 27 (p-value = $1.05e^{-11}$; adjusted $R^2 = 0.975$). Using this model, we inferred a MMR of 10.372 mL $O_2\ h^{-1}\ g^{-0.67}$ (7.676–14.016 mL $O_2\ h^{-1}\ g^{-0.67}$) for *Pelagosaurus typus* MNHN.F.RJN470 (Figure 9). A leave-one-out cross-validation test showed that, for extant species, predicted values are not significantly different from observed values ($p = 0.798$).

4 | DISCUSSION

Pelagosaurus typus MNHN.F.RJN470 had a BM of 6.435 kg (5.112–8.137 kg) and a maximum diaphyseal femoral diameter of 11.49 mm. MNHN.F.RJN463 was slightly smaller (diameter = 10.01 mm) and had an individual age of at least 5 years old. These specimens were used to elucidate the lifestyle and to perform an integrative paleophysiological analysis of *Pelagosaurus typus*.

4.1 | Lifestyle

Was *Pelagosaurus typus* a pelagic organism that used to go out of the water only for reproduction like marine turtles, or it was semiaquatic and used to spend time out of the water for thermoregulatory basking like extant crocodiles? To answer this question, we tested whether

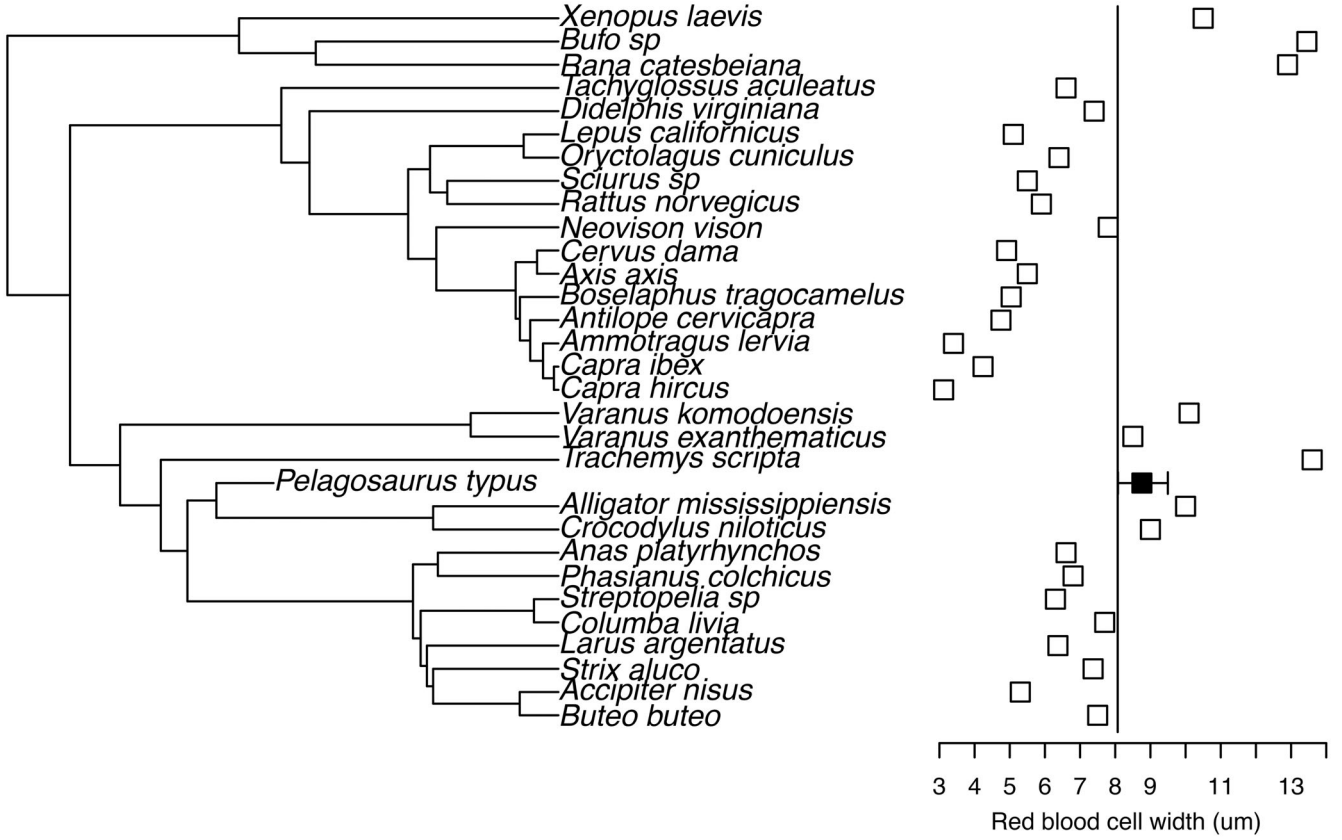

FIGURE 7 Red blood cell sizes quantified in a sample of extant amniotes and inferred in *Pelagosaurus typus* using a set of phylogenetic eigenvectors and the harmonic mean of bone vascular canal diameter (sensu Huttenlocker & Farmer, 2017). Dataset analyzed by Cubo et al. (2023) available in Dryad at Cubo et al. (2022).

the lifestyle (aquatic, amphibious, terrestrial) has an effect on parameters of the femoral compactness profiles using the sample of 155 species of amniotes published by Quémeneur et al. (2013) (to which we added three Crocodylia), and phylogenetic ANOVA (Garland et al., 1993). We found that lifestyle had a significant effect on the variation of P. This parameter indicates the position of the transition area between the medulla and the cortical regions (Quémeneur et al., 2013). It has low values when the bone cortex is thick, as an adaptation to aquatic lifestyle, and high values when the bone cortex is thin, the typical condition of terrestrial animals. In contrast, the S parameter (proportional to the relative width of the transition zone between the medulla and the cortical regions, Quémeneur et al., 2013) and the compactness could not be tested because the conditions of normal distribution and/or homoscedasticity were not verified. Thus, only the P parameter will be discussed.

In the classification of Quémeneur et al. (2013), aquatic species "display advanced morphological specializations for swimming, and their foraging activity occurs exclusively in water," whereas amphibious species "do not show advanced morphological specializations for swimming and remain able to forage on land." The values measured in *Pelagosaurus typus* MNHN.F.RJN470 left femur and MNHN.F.RJN463 right femur were significantly higher than the mean value of the aquatic group ($p = 0.0003$) but not significantly different from the mean value of the amphibious group ($p = 0.093$). Thus, *P. typus* was an amphibious thalattosuchian presumably able to wander over land (Ősi et al., 2018; Pierce & Benton, 2006; Scavezzoni et al., 2024). We hypothesize that (i) the foraging activity of *Pelagosaurus typus* occurs exclusively in water (as suggested by the skull and teeth morphology; Ősi et al., 2018; Pierce & Benton, 2006), and (ii) its P parameter is significantly different from the aquatic group because *Pelagosaurus* used to spend time out of the water, as suggested by the presence of osteoderms with highly developed ornamentation (Figure 1, this study; Ősi et al., 2018; Pierce & Benton, 2006) probably involved in thermoregulatory basking (Clarac & Quilhac, 2019; Johnson, 1974; Johnson et al., 1976, 1978). The presence of a preorbital expansion of the nasal cavity has been interpreted as an osteological

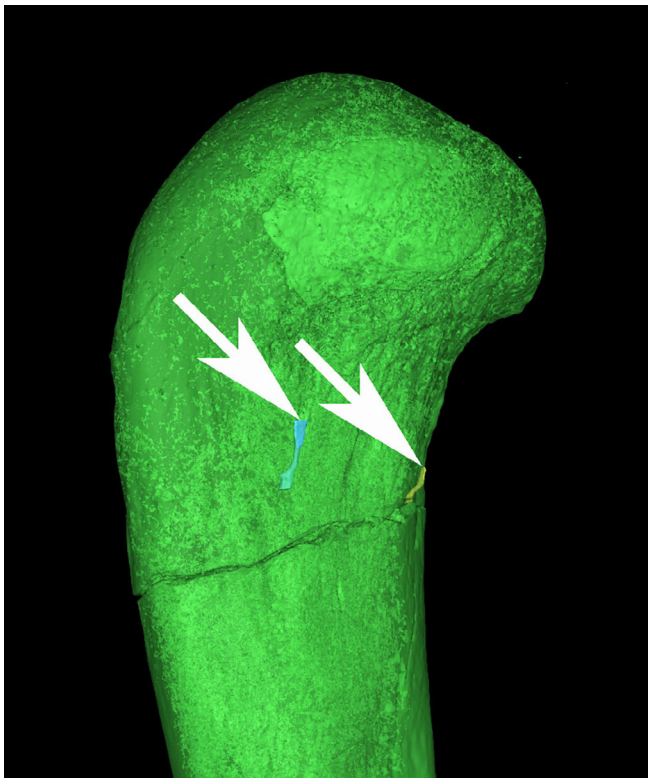

FIGURE 8 CT-scan of left femur MNHN.F.RJN470 in ventral view (anterior part on the right). White arrows point to the openings of the two nutrient foramina.

correlate of a salt gland suggesting that *Pelagosaurus* had a marine lifestyle (Pierce et al., 2017).

4.2 | Thermometabolism

The mass-independent RMR inferred for *Pelagosaurus typus* is higher than those measured in the sample of extant ectothermic amniotes (lizards, turtles, and crocodiles) (Figure 5). At first sight these results may suggest that the thermometabolism of the non-metriorhynchid metriorhynchoid *Pelagosaurus* looks like the "unachieved" or "incomplete" endothermy inferred by Séon et al. (2020) for metriorhynchids. However, analysis of vascular canal diameter (as a proxy of *Pelagosaurus* red blood cell size) refutes this hypothesis (Figure 6). The probability of endothermy obtained using the harmonic mean of *Pelagosaurus* vascular canal diameter and the predictive model (Equation 2, this article) published by Cubo et al. (2023) is $p = 0.27$ (Figure 6). This probability of endothermy is lower than the cut-off probability ($p = 0.59$) separating endotherms from ectotherms (Cubo et al., 2023). We inferred red blood cell width to further investigate *Pelagosaurus* thermometabolism. In *Pelagosaurus,* red blood cell width confidence interval excludes (it is higher than) the line separating endotherms (with small red blood cells) from ectotherms (with large ones; Figure 7). Faure-Brac et al. (2024) proposed a new model to discuss endothermy, called "endothermic engine." According to this model, endothermy is a by-product of tachymetabolism, the latter needing a certain set of adaptations to be sustained. One of the main adaptations of the circulatory system required to sustain tachymetabolism is a small size of erythrocytes (Cubo et al., 2023; Faure-Brac et al., 2024; Huttenlocker & Farmer, 2017; Snyder & Sheafor, 1999; Soslau, 2020): without such small red blood cells, tachymetabolism and, therefore, endothermy, cannot be maintained. Therefore, when conclusions about the thermometabolism drawn using RMR inferences and RBC size inferences are not congruent (as it was the case in the present study), then the latter should always be preferred. This is because high RMR is a collateral effect of endothermy whereas there is a causal relationship between RBC size and thermometabolism (the presence of small RBC is a necessary condition for endothermy). Thus, we conclude that *Pelagosaurus typus* had probably an ectothermic thermometabolism.

4.3 | Hunting behavior

According to Pierce and Benton (2006), "the presence of large laterally placed eyes and a long, thin, gracile body are reminiscent of a pursuit predator, rather than a predator that sits and waits at the water surface." However, our results challenge this suggestion. *Pelagosaurus typus* had a mass-independent MMR of 10.372 mL O_2 h^{-1} $g^{-0.67}$ (7.676–14.016 mL O_2 h^{-1} $g^{-0.67}$). Considering that specimen MNHN.F.RJN470 probably had a residual growth (as it was slightly larger than MNHN.F.RJN463, and the latter was still growing), this MMR may be a realistic estimation for subadults, but an overestimation for adults because foramen size is strongly related to bone growth due to the increased energy/oxygen demands in growing animals (Hu et al., 2018). The inferred value is similar to those measured in the sit-and wait ambush predators *Alligator mississippiensis*, *Crocodylus niloticus*, and *C. porosus* (Figure 9) but lower than those quantified in active hunters like *Varanus gouldii* and *Varanus salvator* and in the sea turtle *Chelonia mydas*, probably because the latter has a more active locomotion mode (Figure 9). We conclude that *Pelagosaurus* may have had a slow sustained subundulatory swimming mode (congruent with the low MMR value inferred in this study), and they may

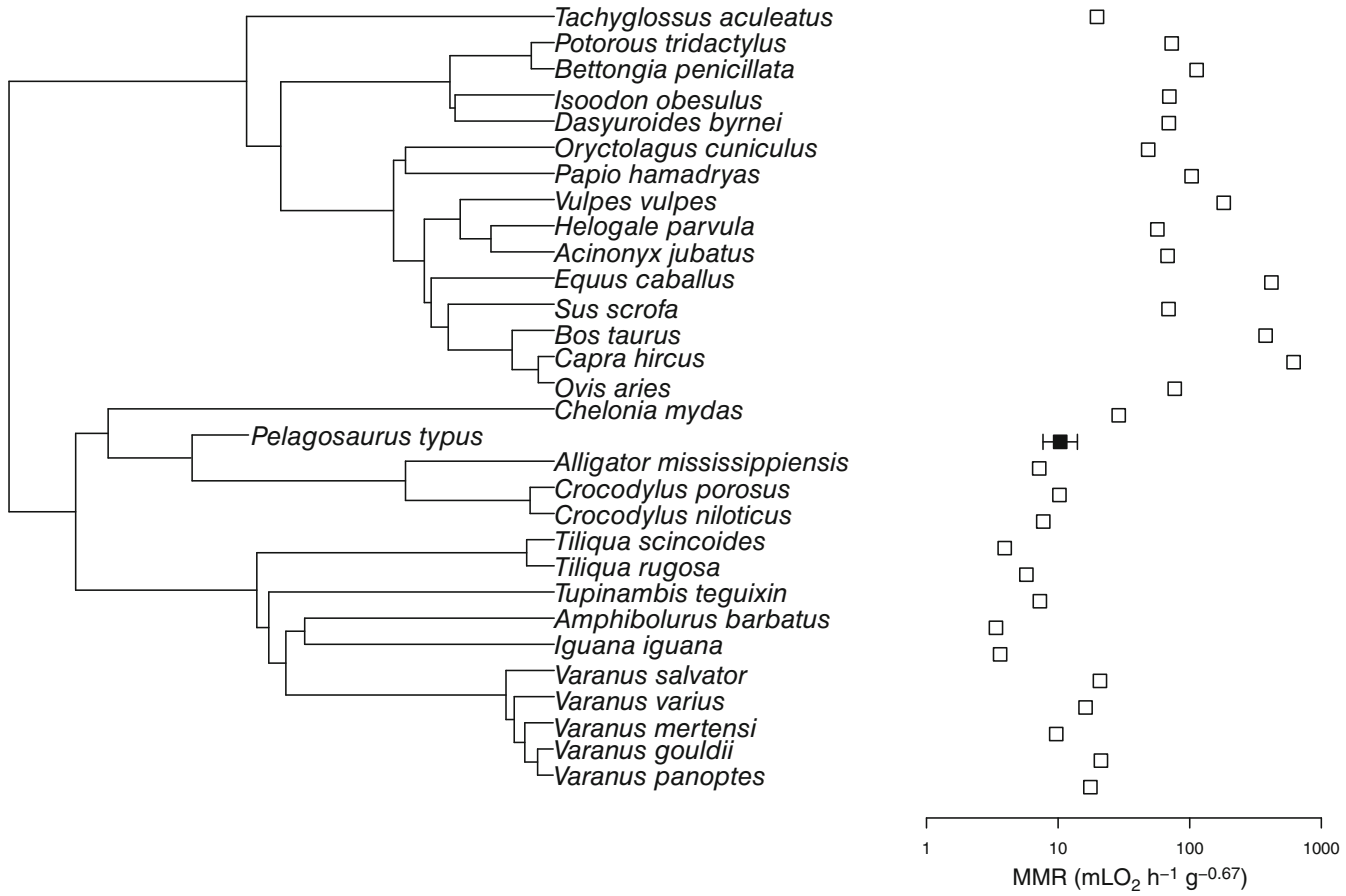

FIGURE 9 Mass-independent maximum metabolic rates quantified in a sample of extant amniotes and inferred in *Pelagosaurus typus* using a set of phylogenetic eigenvectors and blood flow rate ($\dot{Q}$, $cm^3\ s^{-1}$; Seymour et al., 2019) computed using nutrient foramina size. Dataset available in Table 2.

have caught preys like gharials (Thorbjarnarson, 1990), using fast sideways sweeping motions of the head (as suggested by Pierce & Benton, 2006).

The aerobic scopes (i.e., the absolute increment between the RMR and the MMR; Bennett & Ruben, 1979) can shed more light on the hunting behavior of *Pelagosaurus*. According to Bennett and Ruben (1979), "there appears to be a consistent linkage between resting and maximal levels of oxygen consumption in the vertebrates. When the animal is in any given physiological state, oxygen consumption may increase on average of only five- to tenfold." The aerobic scope computed for *Pelagosaurus typus* is: 10.372 mL O_2 h^{-1} $g^{-0.67}$/1.513 mL O_2 h^{-1} $g^{-0.67}$ = 6.86. When compared with extant sauropsids of our sample, the aerobic scope of *Pelagosaurus typus* (i) is higher than that reported by Bennett and Ruben (1979) in the almost motionless lepidosaur *Iguana iguana* (MMR = 9 mL O_2 min^{-1}/1000 $g^{0.67}$; RMR = 2 mL O_2 min^{-1}/1000 $g^{0.67}$; aerobic scope = 4.5); (ii) it is lower than that measured by Crispin (2014) in the active hunter *V. gouldii* (MMR = 155.69 mL O_2h^{-1}/674 $g^{0.67}$; SMR = 19.19 mL O_2h^{-1}/674 $g^{0.67}$; aerobic scope = 8.11); and (iii) it is slightly higher than that reported by Seymour (personal communication) in the sit-and-wait predator *C. porosus* "The ratio of MMR to SMR is (6.56/1.01 = 6.5)." These results are further evidence suggesting that *Pelagosaurus typus* was not a high-speed pursuit hunter like metriorhynchids, but had a feeding behavior closer to that of extant gharials (Thorbjarnarson, 1990).

In conclusion, the two specimens analyzed were probably subadults, of at least 5 years old and with a BM of about 6.4 kg; they were ectotherms, had a semiaquatic marine lifestyle and were not active predators. The slender snout of *Pelagosaurus*, similar to the long snout of the specialized fish-eater *Gavialis gangeticus*, suggests a similar diet (a hypothesis supported by the stomach content of some fossils; Pierce & Benton, 2006), and probably similar feeding habits, with patient waiting for fish in shallow waters, or with slow sustained subundulatory swimming, and rapid lateral movement of the head to capture prey (Singh, 1995, 2018), a kind of ambush predator. Future mass-independent MMR comparisons of

G. gangeticus, other extant species, *P. typus*, its close relatives teleosauroid thalattosuchians and derived metriorhynchids (assumed to be more active hunters), should be carried out. They could help in assessing a possible transition from ambush predators (*Pelagosaurus*) to supposed active hunters (metriorhynchids).

5 | CAVEATS

The conclusions outlined above can be biased because of one or several of the assumptions and postulates listed below can be flawed. Future research in the field will contribute to control for the factors underlying them and produce more robust conclusions. First, we assumed a strong correlation between nutrient foramina size and artery lumen size. However, to model actual blood flow rates, we need to understand the relationship between these variables because this relationship can be dependent upon the blood pressure, the taxonomic group, and other factors. Hu et al. (2021) made progress in this direction by analyzing the relationship between chicken femoral nutrient foramen and femoral nutrient artery lumen size. Similar studies in crocodiles and related taxa may contribute to obtain more realistic results. Second, RMRs vary during ontogeny. The reference dataset for RMR as well as for the histological proxies used to infer them was measured in a sample of extant species composed of juveniles near the age of maximum growth rate. Consistently, we performed measurements of the histological variables (osteocyte density and RPOA) in the deep cortex of *Pelagosaurus* formed when the organism was near the age of maximum growth rate. Third, Quémeneur et al. (2013) based their analyses on adult specimens but the *Pelagosaurus* specimens analyzed here were subadults. We assumed that these age differences do not have an effect on lifestyle inferences, but this postulate deserves to be tested in future studies.

AUTHOR CONTRIBUTIONS

Jorge Cubo: Conceptualization; formal analysis; investigation; writing – original draft. **Mariana V. A. Sena:** Investigation; writing – review and editing. **Romain Pellarin:** Investigation; writing – review and editing. **Mathieu G. Faure-Brac:** Investigation; writing – review and editing. **Paul Aubier:** Investigation; writing – review and editing. **Cassandra Cheyron:** Investigation; writing – review and editing. **Stéphane Jouve:** Writing – review and editing. **Ronan Allain:** Writing – review and editing. **Nour-Eddine Jalil:** Writing – review and editing.

ACKNOWLEDGMENTS

The authors thank Lilian Cazes and Philippe Loubry for having taken the pictures shown in Figures 1 and 2, Hayat Lamrous for the preparation of the thin sections shown in Figure 3, Marta Bellato for having performed the CT-scan shown in Figure 8 at the platform AST-RX of the Paris Muséum national d'Histoire naturelle (MNHN), Damien Germain for allowing access to the thin sections of the vertebrate hard tissues histological collection of the MNHN and Michela M. Johnson and two other anonymous reviewers for their constructive comments.

ORCID

Jorge Cubo https://orcid.org/0000-0002-8160-779X
Mariana V. A. Sena https://orcid.org/0000-0003-4708-999X
Mathieu G. Faure-Brac https://orcid.org/0000-0003-1099-6000

REFERENCES

Araújo, R., David, R., Benoit, J., Lungmus, J. K., Stoessel, A., Barrett, P. M., Maisano, J. A., Ekdale, E., Orliac, M., Luo, Z. X., Martinelli, A. G., Hoffman, E. A., Sidor, C. A., Martins, R. M. S., Spoor, F., & Angielczyk, K. D. (2022). Inner ear biomechanics reveals a Late Triassic origin for mammalian endothermy. *Nature*, *607*, 726–731. https://doi.org/10.1038/s41586-022-04963-z

Bal, N. C., & Periasamy, M. (2020). Uncoupling of sarcoendoplasmic reticulum calcium ATPase pump activity by sarcolipin as the basis for muscle non-shivering thermogenesis. *Philosophical Transactions of the Royal Society of London. Series B, Biological Sciences*, *375*, 20190135. https://doi.org/10.1098/rtsb.2019.0135

Bennett, A. F., & Dawson, W. R. (1976). Metabolism. In C. Gans & W. R. Dawson (Eds.), *Biology of Reptilia* (Vol. 5, pp. 127–223). Academic Press.

Bennett, A. F., & Ruben, J. A. (1979). Endothermy and activity in vertebrates. *Science*, *206*, 649–654.

Bernard, A., Lécuyer, C., Vincent, P., Amiot, R., Bardet, N., Buffetaut, E., Cuny, G., Fourel, F., Martineau, F., Mazin, J. M., & Prieur, A. (2010). Regulation of body temperature by some Mesozoic marine reptiles. *Science*, *328*, 1379–1382. https://doi.org/10.1126/science.1187443

Clarac, F., & Quilhac, A. (2019). The crocodylian skull and osteoderms: A functional exaptation to ectothermy? *Zoology*, *132*, 31–40. https://doi.org/10.1016/j.zool.2018.12.001

Crispin, T. S. (2014). The evolution of metabolic rate in terrestrial ectotherms. The University of Queensland. PhD dissertation.

Cubo, J., Aubier, P., Faure-Brac, M. G., Martet, G., Pellarin, R., Pelletan, I., & Sena, M. V. A. (2022). Paleohistological inferences of thermometabolic regimes in Notosuchia [Dataset]. Dryad. https://doi.org/10.5061/dryad.80gb5mktb

Cubo, J., Aubier, P., Faure-Brac, M. G., Martet, G., Pellarin, R., Pelletan, I., & Sena, M. V. A. (2023). Paleohistological inferences of thermometabolic regimes in Notosuchia (Pseudosuchia: Crocodylomorpha) revisited. *Paleobiology*, *49*(2), 342–352.

Cubo, J., & Jalil, N.-E. (2019). Bone histology of *Azendohsaurus laaroussii*: Implications for the evolution of thermometabolism in Archosauromorpha. *Paleobiology*, *45*, 317–330.

Cubo, J., Le Roy, N., Martinez-Maza, C., & Montes, L. (2012). Paleohistological estimation of bone growth rate in extinct archosaurs. *Paleobiology*, *38*, 335–349.

Cubo, J., Sena, M. V. A., Aubier, P., Houee, G., Claisse, P., Faure-Brac, M. G., Allain, R., Andrade, R. C. L. P., Sayão, J. M., & Oliveira, G. R. (2020). Were Notosuchia (Pseudosuchia: Crocodylomorpha) warm-blooded? A palaeohistological analysis suggests ectothermy. *Biological Journal of the Linnean Society*, *131*, 154–162.

de Buffrénil, V., Laurin, M., & Jouve, S. (2021). Archosauromorpha: The Crocodylomorpha. In V. de Buffrénil, A. de Ricqlès, L. Zylberberg, K. Padian, M. Laurin, & A. Quilhac (Eds.), *Vertebrate skeletal histology and paleohistology* (pp. 486–510). CRC Press.

de Buffrénil, V., Quilhac, A., & Castanet, J. (2021). Cyclical growth and skeletochronology. In V. de Buffrénil, A. de Ricqlès, L. Zylberberg, K. Padian, M. Laurin, & A. Quilhac (Eds.), *Vertebrate skeletal histology and paleohistology* (pp. 626–644). CRC Press.

Fabbri, M., Navalón, G., Benson, R. B. J., Pol, D., O'Connor, J., Bhullar, B. S., Erickson, G. M., Norell, M. A., Orkney, A., Lamanna, M. C., Zouhri, S., Becker, J., Emke, A., Dal Sasso, C., Bindellini, G., Maganuco, S., Auditore, M., & Ibrahim, N. (2022). Subaqueous foraging among carnivorous dinosaurs. *Nature*, *603*, 852–857. https://doi.org/10.1038/s41586-022-04528-0

Faure-Brac, M. G., Amiot, R., de Muizon, C., Cubo, J., & Lécuyer, C. (2022). Combined paleohistological and isotopic inferences of thermometabolism in extinct Neosuchia, using *Goniopholis* and *Dyrosaurus* (Pseudosuchia: Crocodylomorpha) as case studies. *Paleobiology*, *48*, 302–323. https://doi.org/10.1017/pab.2021.34

Faure-Brac, M. G., & Cubo, J. (2020). Were the synapsids primitively endotherms? A palaeohistological approach using phylogenetic eigenvector maps. *Philosophical Transactions of the Royal Society of London. Series B, Biological Sciences*, *375*, 20190138. https://doi.org/10.1098/rstb.2019.0138

Faure-Brac, M. G., Woodward, H. N., Aubier, P., & Cubo, J. (2024). On the origins of endothermy in amniotes. *iScience*, *27*, 109375. https://doi.org/10.1016/j.isci.2024.109375

Fernandez, M., & Gasparini, Z. (2008). Salt glands in the Jurassic metriorhynchid *Geosaurus*: Implications for the evolution of osmoregulation in Mesozoic marine crocodyliforms. *Naturwissenschaften*, *95*, 79–84. https://doi.org/10.1007/s00114-007-0296-1

Fleischle, C., Wintrich, T., & Sanders, P. M. (2018). Quantitative histological models suggest endothermy in plesiosaurs. *PeerJ*, *6*, e4955.

Gardner, J. D., Laurin, M., & Organ, C. L. (2020). The relationship between genome size and metabolic rate in extant vertebrates. *Philosophical Transactions of the Royal Society of London. Series B, Biological Sciences*, *375*, 20190146. https://doi.org/10.1098/rstb.2019.0146

Garland, T., Dickerman, A. W., Janis, C. M., & Jones, J. A. (1993). Phylogenetic analysis of covariance by computer simulation. *Systematic Biology*, *42*, 265–292.

Girondot, M., & Laurin, M. (2003). Bone profiler: A tool to quantify, model and statistically compare bone section compactness profiles. *Journal of Vertebrate Paleontology*, *23*, 458–461. https://doi.org/10.1671/0272-4634(2003)023[0458:BPATTQ]2.0.CO;2

Gônet, J., Laurin, M., & Girondot, M. (2021). BoneProfileR: The next step to quantify, model and statistically compare bone section compactness profiles. *Palaeontologica Electronica*, *25*(1), a12. https://doi.org/10.26879/1194

Grigg, G., Nowack, J., Bicudo, J. E. P. W., Bal, N. C., Woodward, H. N., & Seymour, R. S. (2022). Whole-body endothermy: Ancient, homologous and widespread among the ancestors of mammals, birds and crocodylians. *Biological Reviews*, *97*, 766–801. https://doi.org/10.1111/brv.12822

Guénard, G., Legendre, P., & Peres-Neto, P. (2013). Phylogenetic eigenvector maps: A framework to model and predict species traits. *Methods in Ecology and Evolution*, *4*, 1120–1131.

Hackländer, K., Arnold, W., & Ruf, T. (2002). Postnatal development and thermoregulation in the precocial European hare (*Lepus europaeus*). *Journal of Comparative Physiology B, Biochemical, Systemic, and Environmental Physiology*, *172*, 183–190.

Hu, Q., Miller, C. V., Snelling, E. P., & Seymour, R. S. (2023). Blood flow rates to leg bones of extinct birds indicate high levels of cursorial locomotion. *Paleobiology*, *49*, 700–711. https://doi.org/10.1017/pab.2023.14

Hu, Q., Nelson, T. J., & Seymour, R. S. (2020). Bone foramen dimensions and blood flow calculation: Best practices. *Journal of Anatomy*, *236*, 357–369.

Hu, Q., Nelson, T. J., & Seymour, R. S. (2021). Morphology of the nutrient artery and its foramen in relation to femoral bone perfusion rates of laying and non-laying hens. *Journal of Anatomy*, *240*, 94–106.

Hu, Q., Nelson, T. J., Snelling, E. P., & Seymour, R. S. (2018). Femoral bone perfusion through the nutrient foramen during growth and locomotor development of western grey kangaroos (*Macropus fuliginosus*). *Journal of Experimental Biology*, *221*, jeb168625.

Hu, Q., Seymour, R., Snelling, E. P., & Wells, R. (2024). Blood flow rate to the femur of extinct kangaroos implies a higher locomotor intensity compared to living hopping macropods. *Journal of Mammalian Evolution*, *31*, 1–8. https://doi.org/10.1007/s10914-023-09701-4

Hua, S., & de Buffrénil, V. (1996). Bone histology as a clue in the interpretation of functional adaptations in the Thalattosuchia (Reptilia, Crocodylia). *Journal of Vertebrate Paleontology*, *16*, 703–717. https://doi.org/10.1080/02724634.1996.10011359

Huttenlocker, A. K., & Farmer, C. G. (2017). Bone microvasculature tracks red blood cell size diminution in Triassic mammal and dinosaur forerunners. *Current Biology*, *27*, 48–54. https://doi.org/10.1016/j.cub.2016.10.012

Ives, A. R., & Garland, T. (2010). Phylogenetic logistic regression for binary dependent variables. *Systematic Biology*, *59*, 9–26.

Janis, C. M., Napoli, J. G., & Warren, D. E. (2020). Palaeophysiology of pH regulation in tetrapods. *Philosophical Transactions of the Royal Society of London. Series B, Biological Sciences*, *375*, 20190131. https://doi.org/10.1098/rstb.2019.0131

Johnson, C. R. (1974). Thermoregulation in crocodilians—I. Head-body temperature control in the papuan-New Guinean crocodiles. *Comparative Biochemistry and Physiology Part A: Physiology*, *49*, 3–28. https://doi.org/10.1016/0300-9629(74)90538-6

Johnson, C. R., Voigt, W. G., & Smith, N. (1978). Thermoregulation in crocodilians—III. Thermal preferenda, voluntary

maxima, and heating and cooling rates in the American alligator, *Alligator mississippiensis*. *Zoological Journal of the Linnean Society*, *62*, 179–188. https://doi.org/10.1111/j.1096-3642.1978.tb01036.x

Johnson, C. R., Webb, G. J. W., & Tanner, C. (1976). Thermoregulation in crocodilians—ii. A telemetric study of body temperature in the Australian crocodiles, *Crocodylus johnstoni* and *Crocodylus porosus*. *Comparative Biochemistry and Physiology Part A: Physiology*, *53*, 143–146. https://doi.org/10.1016/S0300-9629(76)80044-8

Johnson, M. M., Young, M. T., & Brusatte, S. L. (2020). The phylogenetics of Teleosauroidea (Crocodylomorpha, Thalattosuchia) and implications for their ecology and evolution. *PeerJ*, *8*, e9808. https://doi.org/10.7717/peerj.9808

Knaus, P. L., van Heteren, A. H., Lungmus, J. K., & Sander, P. M. (2021). High blood flow into the femur indicates elevated aerobic capacity in synapsids since the Synapsida-Sauropsida Split. *Frontiers in Ecology and Evolution*, *9*, 751238. https://doi.org/10.3389/fevo.2021.751238

Kumar, S., Suleski, M., Craig, J. M., Kasprowicz, A. E., Sanderford, M., Li, M., Stecher, G., & Hedges, S. B. (2022). TimeTree 5: An expanded resource for species divergence times. *Molecular Biology and Evolution*, *39*(8), msac174. https://doi.org/10.1093/molbev/msac174

Legendre, L. J., Guénard, G., Botha-Brink, J., & Cubo, J. (2016). Palaeohistological evidence for ancestral high metabolic rate in archosaurs. *Systematic Biology*, *65*, 989–996.

Mauget, C., Mauget, R., & Sempéré, A. (1999). Energy expenditure in European roe deer fawns during the suckling period and its relationship with maternal reproductive cost. *Canadian Journal of Zoology-Revue Canadienne De Zoologie*, *77*, 389–396.

Mitchell, J., Legendre, L. J., Lefèvre, C., & Cubo, J. (2017). Bone histological correlates of soaring and high-frequency flapping flight in the furculae of birds. *Zoology*, *122*, 90–99.

Montes, L., Le Roy, N., Perret, M., de Buffrénil, V., Castanet, J., & Cubo, J. (2007). Relationships between bone growth rate, body mass and resting metabolic rate in growing amniotes: A phylogenetic approach. *Biological Journal of the Linnean Society*, *92*, 63–76. https://doi.org/10.1111/j.1095-8312.2007.00881.x

Myhrvold, N. P., Baumgart, S. L., Vidal, D., Fish, F. E., Henderson, D. M., Saitta, E. T., & Sereno, P. C. (2024). Diving dinosaurs? Caveats on the use of bone compactness and pFDA for inferring lifestyle. *PLoS One*, *19*, e0298957. https://doi.org/10.1371/journal.pone.0298957

Newham, E., Gill, P. G., Brewer, P., Benton, M. J., Fernandez, V., Gostling, N. J., Haberthür, D., Jernvall, J., Kankaanpää, T., Kallonen, A., Navarro, C., Pacureanu, A., Richards, K., Brown, K. R., Schneider, P., Suhonen, H., Tafforeau, P., Williams, K. A., Zeller-Plumhoff, B., & Corfe, I. J. (2020). Reptile-like physiology in Early Jurassic stem-mammals. *Nature Communications*, *11*, 5121. https://doi.org/10.1038/s41467-020-18898-4

Olivier, C., Houssaye, A., Jalil, N.-E., & Cubo, J. (2017). First palaeohistological inference of resting metabolic rate in an extinct synapsid, *Moghreberia nmachouensis* (Therapsida: Anomodontia). *Biological Journal of the Linnean Society*, *121*, 409–419.

Organ, C. L., & Shedlock, A. M. (2009). Palaeogenomics of pterosaurs and the evolution of small genome size in flying vertebrates. *Biology Letters*, *5*, 47–50. https://doi.org/10.1098/rsbl.2008.0491

Organ, C. L., Shedlock, A. M., Meade, A., Pagel, M., & Edwards, S. V. (2007). Origin of avian genome size and structure in non-avian dinosaurs. *Nature*, *446*, 180–184. https://doi.org/10.1038/nature05621

Ősi, A., Young, M. T., Galácz, A., & Rabi, M. (2018). A new large-bodied thalattosuchian crocodyliform from the Lower Jurassic (Toarcian) of Hungary, with further evidence of the mosaic acquisition of marine adaptations in Metriorhynchoidea. *PeerJ*, *6*, e4668. https://doi.org/10.7717/peerj.4668

Pierce, S., & Benton, M. (2006). *Pelagosaurus typus* Bronn, 1841 (Mesoeucrocodylia: Thalattosuchia) from the Upper Lias (Toarcian, Lower Jurassic) of Somerset, England. *Journal of Vertebrate Paleontology*, *26*, 621–635.

Pierce, S. E., Williams, M., & Benson, R. B. J. (2017). Virtual reconstruction of the endocranial anatomy of the early Jurassic marine crocodylomorph *Pelagosaurus typus* (Thalattosuchia). *PeerJ*, *5*, e3225. https://doi.org/10.7717/peerj.3225

Pochat-Cottilloux, Y., Martin, J. E., Faure-Brac, M. G., Jouve, S., de Muizon, C., Cubo, J., Lécuyer, C., Fourel, F., & Amiot, R. (2023). A multi-isotopic study reveals the palaeoecology of a sebecid from the Paleocene of Bolivia. *Palaeogeography, Palaeoclimatology, Palaeoecology*, *625*, 111667. https://doi.org/10.1016/j.palaeo.2023.111667

Pontzer, H., Allen, V., & Hutchinson, J. R. (2009). Biomechanics of running indicates endothermy in bipedal dinosaurs. *PLoS ONE*, *4*(11), e7783. https://doi.org/10.1371/journal.pone.0007783

Pyron, R. A., Burbrink, F. T., & Wiens, J. J. (2013). A phylogeny and revised classification of Squamata, including 4161 species of lizards and snakes. *BMC Evolutionary Biology*, *13*, 93. https://doi.org/10.1186/1471-2148-13-93

Quémeneur, S., de Buffrénil, V., & Laurin, M. (2013). Microanatomy of the amniote femur and inference of lifestyle in limbed vertebrates. *Biological Journal of the Linnean Society*, *109*, 644–655. https://doi.org/10.1111/bij.12066

R Core Team. (2023). R: A language and environment for statistical computing [computer software manual]. Vienna, Austria. Retrieved from https://www.R-project.org

Revell, L. (2024). phytools 2.0: An updated R ecosystem for phylogenetic comparative methods (and other things). *PeerJ*, *12*, e16505. https://doi.org/10.7717/peerj.16505

Rowland, L. A., Bal, N. C., & Periasamy, M. (2015). The role of skeletal-muscle based thermogenic mechanisms in vertebrate endothermy. *Biological Reviews*, *90*, 1279–1297. https://doi.org/10.1111/brv.12157

Scavezzoni, I., Fischer, V., Johnson, M. M., & Jouve, S. (2024). Form and function of the pelvic girdle of Thalattosuchia and Dyrosauridae (Crocodyliformes). *Geodiversitas*, *46*, 135–326.

Seltmann, M. W., Ruf, T., & Röedel, H. G. (2009). Effects of body mass and huddling on resting metabolic rates of post-weaned European rabbits under different simulated weather conditions. *Functional Ecology*, *23*, 1070–1080.

Sena, M. V. A., Montefeltro, F. C., Marinho, T. S., Langer, M. C., Fachini, T. S., Piacentini Pinheiro, A. E., Machado, A. S., Lopes, R. T., Pellarin, R., Sayão, J. M., Oliveira, G. R., & Cubo, J. (2023). The cost of living in Notosuchia (Crocodyliformes, Mesoeucrocodylia). *Palaeogeography,*

Palaeoclimatology, Palaeoecology, *632*, 111855. https://doi.org/10.1016/j.palaeo.2023.111855

Séon, N., Amiot, R., Martin, J. E., Young, M. T., Middleton, H., Fourel, F., Picot, L., Valentin, X., & Lécuyer, C. (2020). Thermophysiologies of Jurassic marine crocodylomorphs inferred from the oxygen isotope composition of their tooth apatite. *Philosophical Transactions of the Royal Society B: Biological Sciences*, *375*, 20190139. https://doi.org/10.1098/rstb.2019.0139

Seymour, R. S. (2013). Maximal aerobic and anaerobic power generation in large crocodiles versus mammals: Implications for dinosaur gigantothermy. *PLoS One*, *8*, e69361.

Seymour, R. S. (2016). Cardiovascular physiology of dinosaurs. *Physiology*, *31*, 430–441. https://doi.org/10.1152/physiol.00016.2016

Seymour, R. S., Bennett-Stamper, C. L., Johnston, S. D., Carrier, D. R., & Grigg, G. C. (2004). Evidence for endothermic ancestors of crocodiles at the stem of archosaur evolution. *Physiological and Biochemical Zoology*, *77*, 1051–1067. https://doi.org/10.1086/422766

Seymour, R. S., Hu, Q., Snelling, E. P., & White, C. R. (2019). Interspecific scaling of blood flow rates and arterial sizes in mammals. *The Journal of Experimental Biology*, *222*, jeb199554. https://doi.org/10.1242/jeb.199554

Seymour, R. S., & Lillywhite, H. B. (2000). Hearts, neck posture and metabolic intensity of sauropod dinosaurs. *Philosophical Transactions of the Royal Society B: Biological Sciences*, *267*, 1883–1887.

Seymour, R. S., Smith, S. L., White, C. R., Henderson, D. M., & Schwarz-Wings, D. (2012). Blood flow to long bones indicates activity metabolism in mammals, reptiles and dinosaurs. *Proceedings of the Biological Sciences*, *279*, 451–456. https://doi.org/10.1098/rspb.2011.0968

Singh, L. A. K. (1995). Food of gharial, *Gavialis gangeticus* (Reptilia, Crocodilia). *Zoo's Print*, *10*, 24–27.

Singh, L. A. K. (2018). *Gharial is a fish-eating crocodile its ecology, behaviour and conservation*. Lambert Academic Publishing.

Snyder, G. K., & Sheafor, B. A. (1999). Red blood cells: Centerpiece in the evolution of the vertebrate circulatory system. *American Zoologist*, *39*, 189–198.

Soslau, G. (2020). The role of the red blood cell and platelet in the evolution of mammalian and avian endothermy. *Journal of Experimental Zoology Part B: Molecular and Developmental Evolution*, *334*, 113–127.

Spindler, F., Lauer, R., Tischlinger, H., & Mäuser, M. (2021). The integument of pelagic crocodylomorphs (Thalattosuchia: Metriorhynchidae). *Palaeontologia Electronica*, *24*(2), a25. https://doi.org/10.26879/1099

Thorbjarnarson, J. B. (1990). Notes on the feeding behavior of the gharial (*Gavialis gangeticus*) under semi-natural conditions. *Journal of Herpetology*, *24*, 99–100.

Tung Ho, L. S., & Ané, C. (2014). A linear-time algorithm for gaussian and non-gaussian trait evolution models. *Systematic Biology*, *63*, 397–408.

Upham, N. S., Esselstyn, J. A., & Jetz, W. (2019). Inferring the mammal tree: Species-level sets of phylogenies for questions in ecology, evolution, and conservation. *PLoS Biology*, *17*, e3000494. https://doi.org/10.1371/journal.pbio.3000494

Villa, A., Abella, J., Alba, D. M., Almécija, S., Bolet, A., Koufos, G. D., Knoll, F., Luján, À. H., Morales, J., Robles, J. M., Sánchez, I. M., & Delfino, M. (2018). Revision of *Varanus marathonensis* (Squamata, Varanidae) based on historical and new material: Morphology, systematics, and paleobiogeography of the European monitor lizards. *PLoS One*, *13*, e0207719. https://doi.org/10.1371/journal.pone.0207719

Wiemann, J., Menéndez, I., Crawford, J. M., Fabbri, M., Gauthier, J. A., Hull, P. M., Norell, M. A., & Briggs, D. E. G. (2022). Fossil biomolecules reveal an avian metabolism in the ancestral dinosaur. *Nature*, *606*, 522–526. https://doi.org/10.1038/s41586-022-04770-6

Woodward, H. N., Aubier, P., de Sena, M. V. A., & Cubo, J. (2025). Evaluating extinct Pseudosuchian body mass estimates using a femur volume-based model. *The Anatomical Record*, *308*(2), 257–265. https://doi.org/10.1002/ar.25452

Young, M. T., Brusatte, S. L., Ruta, M., & De Andrade, M. B. (2010). The evolution of Metriorhynchoidea (Mesoeucrocodylia, Thalattosuchia): An integrated approach using geometric morphometrics, analysis of disparity, and biomechanics. *Zoological Journal of the Linnean Society*, *158*, 801–859. https://doi.org/10.1111/j.1096-3642.2009.00571.x

Zurano, J. P., Magalhães, F. M., Asato, A. E., Silva, G., Bidau, C. J., Mesquita, D. O., & Costa, G. C. (2019). Cetartiodactyla: Updating a time-calibrated molecular phylogeny. *Molecular Phylogenetics and Evolution*, *133*, 256–262. https://doi.org/10.1016/j.ympev.2018.12.015

How to cite this article: Cubo, J., Sena, M. V. A., Pellarin, R., Faure-Brac, M. G., Aubier, P., Cheyron, C., Jouve, S., Allain, R., & Jalil, N.-E. (2025). Integrative paleophysiology of the metriorhynchoid *Pelagosaurus typus* (Pseudosuchia, Thalattosuchia). *The Anatomical Record*, *308*(2), 394–411. https://doi.org/10.1002/ar.25548